Hydrol. Earth Syst. Sci., 28, 5311–5329, 2024
https://doi.org/10.5194/hess-28-5311-2024

Hydrology and Earth System Sciences
Open Access
EGU

The role of neotectonics and climate variability in the Pleistocene-to-Holocene hydrological evolution of the Fuente de Piedra playa lake (southern Iberian Peninsula)

Alejandro Jiménez-Bonilla[1], Lucía Martegani[2,3], Miguel Rodríguez-Rodríguez[1], Fernando Gázquez[2,3], Manuel Díaz-Azpíroz[1], Sergio Martos[4], Klaus Reicherter[5], and Inmaculada Expósito[1]

[1]Department of Physics, Chemistry and Natural Systems, Pablo de Olavide University, 41013 Seville, Spain
[2]Department of Biology and Geology, Water Resources and Environmental Geology Research Group, University of Almería, 04120 Almería, Spain
[3]Andalusian Centre for Global Change – Hermelindo Castro. ENGLOBA, University of Almería, 04120 Almería, Spain
[4]Geological Survey of Spain (IGME), 28003 Madrid, Spain
[5]Institute of Neotectonics and Natural Hazards, RWTH Aachen University, 52062 Aachen, Germany

Correspondence: Alejandro Jiménez-Bonilla (ajimbon@upo.es)

Received: 10 May 2024 – Discussion started: 8 July 2024
Revised: 29 September 2024 – Accepted: 30 October 2024 – Published: 12 December 2024

Abstract. Playa lakes that developed in semi-arid regions are sensitive to water input reductions, which may be influenced not only by climate changes and human management, but also by changes in the size of the watershed. We conducted an interdisciplinary study combining structural, geomorphic, sedimentological, mineralogical and hydrological analyses to better understand the evolution of the Fuente de Piedra (FdP) playa lake in southern Spain. By using previously published temperature and precipitation reconstructions, we assessed the potential evapotranspiration and runoff to estimate the maximum lake level during the FdP playa-lake lifespan ($>$ 35 ka). Our results indicate that the FdP playa-lake level never exceeded 5 m, although deposits at its north-eastern margin are up to 15 m above the current lake bed at present. These lacustrine deposits are slightly tilted towards the south-west. The electrical conductivity profiles of groundwater on the FdP's shore and in its surroundings reveal a more pronounced interface between brackish water and brine in the northern part of the basin compared to the southern part. This implies that saline water once occupied the northern playa-lake margin in an area that is hardly ever flooded at present. The presence of reworked gypsum in the sedimentary sequence of the southern margin (down to a depth of 14 m) indicates substantial erosion of prior gypsum deposits that are possibly redistributed from northern deposition areas. Altogether, our data suggest a south-westerly displacement of the playa-lake depocentre caused by an uplift of the eastern area and subsidence of the south-western area. This shift is congruent with the combined effect of both the La Nava sinistral–normal fault and the Las Latas dextral–normal fault at the eastern and southern margins of the FdP playa lake. Consequently, the FdP flooded surface mostly remained constant and in equilibrium with climate variables and its watershed along its lifespan. The south-westerly displacement of the flooded surface was provoked by the recent tectonic activity.

1 Introduction

Saline playa lakes develop in semi-arid to arid regions, where precipitation is considerably lower than evapotranspiration, leading to negative water balances. The water inputs are direct precipitation and runoff from the catchment, while the water outputs are evapotranspiration and infiltration. Slight changes in the water balance lead to significant seasonal and interannual water level variability.

Under negative water balance conditions, the average flooded surface shrinks, eventually giving rise to complete desiccation and playa-lake disappearance (Moral et

al., 2013). Several factors control the change in the water discharge to playa lakes, such as groundwater extractions for agricultural purposes (Rodríguez-Rodríguez et al., 2015) or climate changes (Schöder et al., 2018; García-Alix et al., 2022). In this regard, variations in temperature and/or precipitation happened naturally over the Quaternary (e.g. Mann et al., 2003; Hughes and Crawford, 2013), resulting in changes in evapotranspiration and lake inputs. In addition, recent studies, which modelled the vertical lake evolution, suggest that anthropogenic climate change during the Late Holocene may have provoked additional changes in lake water input and evapotranspiration (e.g. Matthews et al., 2008). The bathymetry of these wetlands is characterised by planar surfaces, and they show low sedimentation rates (e.g. García-Alix et al., 2022). In general, they are ephemeral water bodies where evaporation leads to the formation of salt crusts during the dry season (e.g. Sánchez-Moral et al., 2002). When these wetlands are dry, they are sensitive to aeolian erosion because of the formation of clay–salt aggregates (Moral Martos, 2016).

Climate changes are recorded in the sedimentary playa-lake register, so playa-lake sediments can provide valuable palaeoclimate information (Roberts et al., 2001; Höbig et al., 2016; Schöder et al., 2018, 2020; Cohen et al., 2022; García-Alix et al., 2022). However, accurate interpretations of their sedimentary records require deep knowledge of the landscape evolution in the surrounding areas, especially those changes related to variations in their catchment size and geometry. Although these changes in both flooded areas and watersheds of playa lakes have been poorly investigated to date, recent studies have demonstrated that such water bodies are quite dynamic, especially those in active orogens (e.g. Berry et al., 2019), where tectonic processes may favour dividing migration and watershed capture, leading to variations in the watershed area (Jiménez-Bonilla et al., 2023a).

The Fuente de Piedra (FdP) playa lake is the largest playa lake within an endorheic area located at the Atlantic–Mediterranean water divide in southern Spain (Figs. 1 and 2). The FdP playa lake remains completely desiccated during the dry season (May to October), except for exceptionally wet interannual periods, when the lake level can reach more than 2 m (Rodríguez-Rodríguez et al., 2016). The FdP watershed developed in a depressed area within the Betics fold-and-thrust belt, which is limited by topographic highs controlled by transpressional shear zones with evidence of moderate Quaternary tectonic activity (Jiménez-Bonilla et al., 2016; 2023a, b). In recent decades, several studies assessed the modern hydrology and palaeohydrological evolution of this endorheic system (e.g. Kohfahl et al., 2008; Höbig et al., 2016; Rodríguez-Rodríguez et al., 2016). These investigations assumed that the FdP playa lake's surface as well as its watershed geometry and extension have remained constant since their origins (at least 35 kyr BP; Höbig et al., 2016). Consequently, variations in the lake-flooded surface had been attributed to palaeoclimate changes. Indeed, presumed Pleistocene lake terraces (10 m above the current lake floor) were reported and interpreted as evidence of lake highstands during humid periods (Höbig et al., 2016).

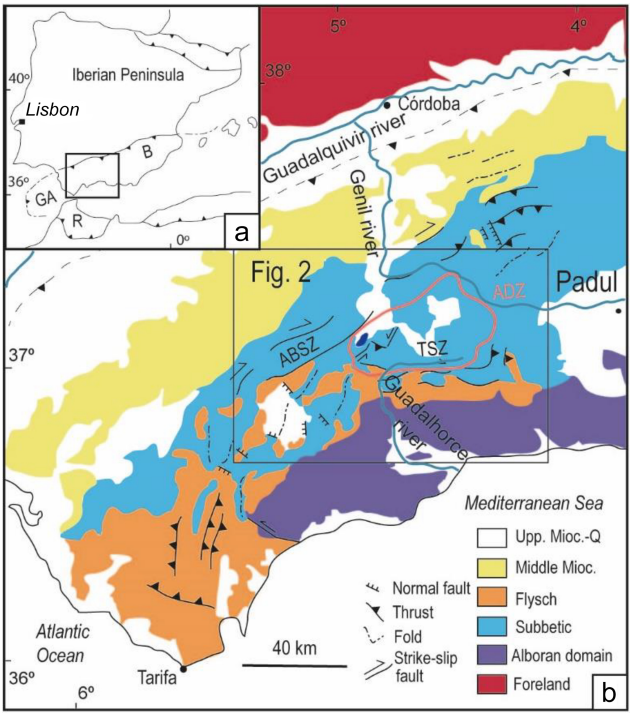

Figure 1. (a) Inset location map. **(b)** Tectonic map of the western Betics showing the Atlantic–Mediterranean water divide and the placement of the Padul peatland, used here for water level calculations (Sect. 3.1). TSZ: Torcal Shear Zone; ABSZ: Algodonales–Badolatosa Shear Zone; ADZ: Antequera Depressed Zone.

Here, we develop an evolution model for the FdP playa lake based on structural, hydrological and sedimentological information. The general aims of this paper are (i) to re-examine the role of Late Quaternary tectonic activity in the FdP playa lake, (ii) to propose an integrated chronology of the FdP playa lake's sediments after careful characterisation of its sediments and tectonic settings and (iii) to investigate the potential impact of climate changes on the lake by modelling the water level over the past 35 kyr based on both lithological and mineralogical variations in the FdP sedimentary sequence and changes in the geometry of the flooded area.

2 Geological setting

The Betic cordillera, which is the northern branch of the Gibraltar arc, is composed of the Neogene collision between the Alborán domain (hinterland) and the South Iberian palaeomargin (Vera, 2004; Fig. 1a). During the westward migration of the Alborán domain, Flysch units were deposited and later sandwiched between both domains. The South Iberian palaeomargin was deformed into the Betics

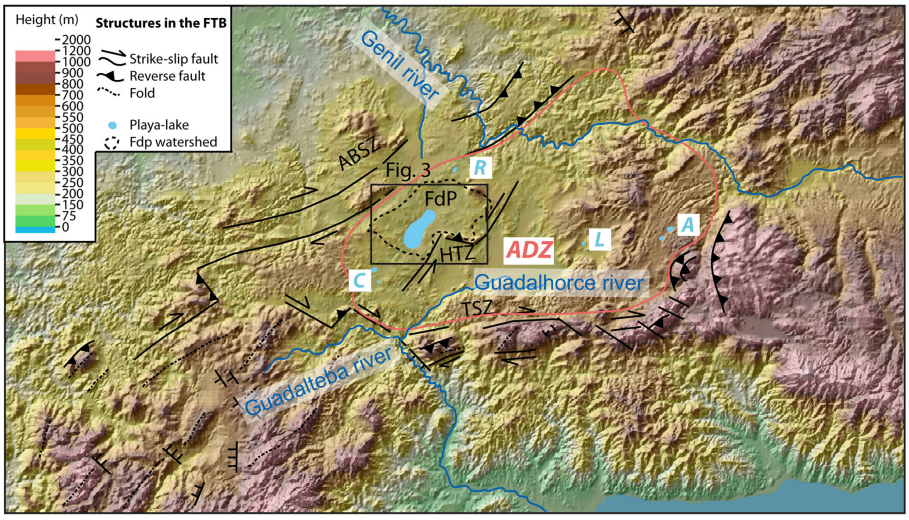

Figure 2. Topographic map and hillshade of the ADZ showing the main playa lakes – FdP (Fuente de Piedra), R (Ratosa), C (Campillos), L (Lomas) and A (Archidona) – and the main structures grouped into three main shear zones: the TSZ, ABSZ and HTZ (Humilladero Transverse Zone).

fold-and-thrust belt, which registers a main, lower and middle Miocene deformation and a late post-Serravallian deformation event responsible for the main current relief. This late deformation is still active along the belt (e.g. Balanya et al., 2012; Jiménez-Bonilla et al., 2015).

2.1 The Antequera Depressed Zone (ADZ)

The study area is the FdP endorheic watershed, which lies in an east–west elongated depressed area in the Betics fold-and-thrust belt. This basinal area, hereafter referred to as the ADZ (Figs. 1 and 2), is limited by mountain ranges which are mainly controlled by two post-Serravallian, dextral transpressive zones: the Algodonales–Badolatosa Shear Zone (ABSZ; Jiménez-Bonilla et al., 2015) to the north-west and the Torcal Shear Zone (TSZ, Díaz-Azpiroz et al., 2014; Barcos et al., 2015) to the south and south-west (Figs. 1 and 2). Both the ABSZ and TSZ show evidence of upper Miocene and recent tectonic activity (Barcos et al., 2015; Díaz-Azpiroz et al., 2020; Jiménez-Bonilla et al., 2023a, b). Both shear zones produce topographic highs located at 600–800 and > 1000 m a.s.l. for the ABSZ and TSZ, respectively (Fig. 2), which drop sharply to the ADZ. The ADZ is characterised by a mostly flat topography at ca. 450 m a.s.l. It includes some scattered reliefs, such as the Humilladero range (Fig. 2), generated by a compressive bridge that links two left-lateral shear zones of the post-Tortonian Humilladero Transverse Zone (HTZ; Fig. 2). Some studies suggest that the ADZ nucleated as an endorheic area after the emersion of this Betics segment in Pliocene to Pleistocene times (Elez et al., 2018, 2020). The ADZ was later captured and partially drained by the Guadalhorce and Guadalteba rivers to the Mediterranean and by the Guadalquivir River network to the Atlantic (Figs. 1 and 2). Thus, the main Quaternary Atlantic–Mediterranean water divide is located in the western Betics, but this is not a sharp feature. In fact, it is a 1 km diffuse area presenting several endorheic basins (Rodríguez-Rodríguez et al., 2010): the FdP watershed, which includes the FdP and La Nava playa lakes; the Campillos (C) endorheic basin, made up of more than 10 playa lakes; the Archidona (A) playa lakes; the Ratosa (R) endorheic basin and the Lomas (L) playa lakes (Fig. 2).

2.2 FdP watershed rocks

The lithological formations that crop out in the FdP watershed (Figs. 1 and 2) belong to the Subbetic units. These Subbetic units are derived from the most internal position of the South Iberian palaeomargin and are made up of Tortonian-to-Messinian shallow marine deposits and Pleistocene-to-Holocene continental deposits (Vera, 2004). The Subbetic units are composed of (1) Triassic clays, gypsum and marls that include isolated dam to hectometre dolostone bodies; (2) Jurassic dolostones and limestones that constitute the main mountain ranges (Sierra de los Caballos in the ABSZ and Sierra de Humilladero in the HTZ; Fig. 3) and (3) Cretaceous-to-Paleogene marls and marly limestones. Recent works interpreted the Triassic rocks outcropping in this area as an allochthonous canopy and the main mountain ranges made up of Jurassic limestones as tectonic windows (Flinch and Soto, 2017, 2022). Upper Miocene shallow marine deposits testify to the progressive shallowing of the ADZ. They are Tortonian-to-Messinian calcarenites and marls (Cruz-Sanjulián, 1991) probably deposited in small-sized basins (Flinch and Soto, 2017). Previous geological maps show that these sediments are deformed by open folds

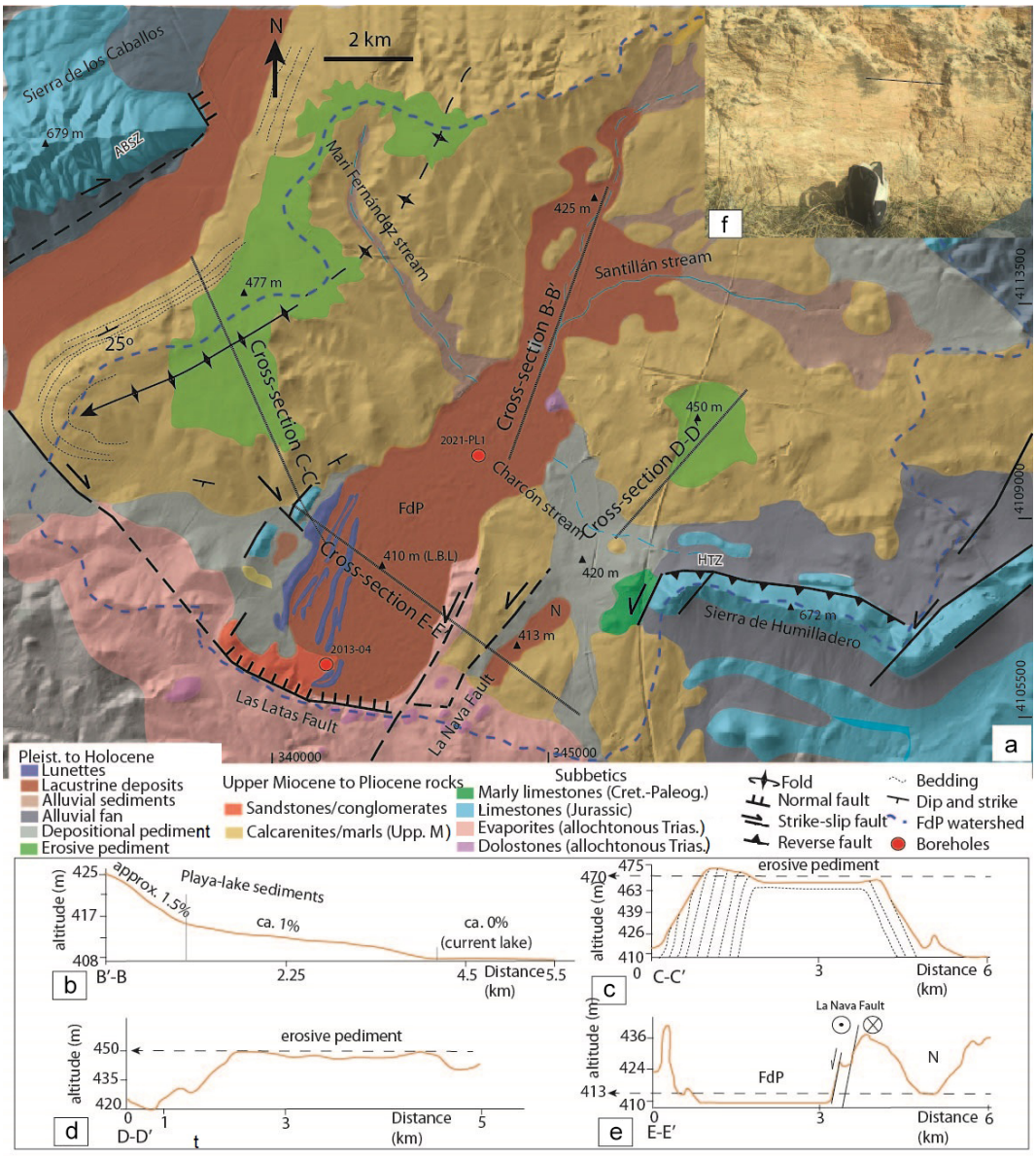

Figure 3. **(a)** Geological map of the FdP playa-lake sediments and their watershed (LBL: lake base level) with the locations of the two drilling cores used in this work. Topographic cross sections showing **(b)** the FdP sediment slope, **(c)** the geometry of an erosive pediment to the west of the FdP playa-lake sediments, **(d)** the geometry of an erosive pediment to the east of the FdP playa-lake sediments, **(e)** the sinistral–normal La Nava fault that separates the FdP and La Nava (N) playa lakes and **(f)** a left-lateral strike–slip fault associated with the La Nava fault.

and faults and often lie unconformably over Subbetic units (Flinch and Soto, 2017, 2022). Pliocene sediments vary from polygenic sandstones associated with beach-like environments to continental conglomerates related to alluvial fans. The sources of these conglomerates and sandstones are located immediately to the south of the TSZ and include Alborán domain clasts of schists, marbles and gneisses together with sandstone and limestone clasts from Flysch and Subbetic units.

Pleistocene-to-Holocene sedimentary sequences are stream-related sediments such as alluvial terraces, alluvial fans and playa-lake-related deposits (e.g. sandy aeolian lunettes and other lacustrine deposits; Fig. 3).

2.3 Hydrological features of the FdP playa lake

The FdP playa lake occupies a conspicuously eccentric location at the south-western edge of a topographically closed watershed of about 150 km^2. The flat surface – flooded seasonally – has a NE–SW elongated ellipsoidal shape (6.8 km

long and 2.5 km wide), which is, in turn, aligned with the Ratosa playa lake to the north-east and the Campillos playa lakes to the south-west of the FdP watershed (Fig. 2). The FdP playa lake is defined as a hyper-saline lake of the Cl–(SO_4)–Na–(Mg)–(Ca) type. The concentrations of dissolved solids range from 18 to 200 g L^{-1} in the surface water (Rodríguez-Rodríguez et al., 2012). The FdP playa lake has a lifespan of at least 26 years and is probably longer than 45 kyr (Höbig et al., 2016). Under natural conditions, the FdP playa lake receives surface and subsurface runoff from its watershed. The outputs only correspond to evapotranspiration (Rodríguez-Rodríguez et al., 2016). In summer, the FdP is completely dry, but minimum piezometric levels under the playa floor range from −20 to −30 cm (Kohfahl et al., 2008). This is consistent with a discharge-type playa lake with a hydrogeological basin that is almost coincident with the surface watershed (Kohfahl et al., 2008). In the past, the playa lake was the lowest part of the hydrogeological basin and also received water inputs from the northern and north-eastern sectors of a spring located in the foothills of the carbonate aquifer of the Mollina mountain range (by means of the Santillán stream; Fig. 3) and, most probably, groundwater inputs from the Sierra de Humilladero mountain range (Figs. 2 and 3), although no springs have been observed in this carbonate aquifer. Both aquifers are intensively exploited at present (e.g. Rodríguez-Rodríguez et al., 2015), but in natural regimes there are estimations of the recharge in both aquifers of 25 %–30 % of the average precipitation in the region (ca. 440 mm yr^{-1}) (Martos-Rosillo et al., 2015). Below the playa lake, a hyper-saline stable groundwater brine has developed via evapotranspiration and convection processes (Kohfahl et al., 2008; Benavente et al., 1993). The high salinity and density of the water in the playa-lake surface favour slow percolation of this brine below the lake. This brine is detached from the fresh groundwater of the aquifer by a freshwater–saltwater interface, similar to that of coastal aquifers, with the playa-lake perimeter being equivalent to the coastal shore. A summary of relevant studies on the hydrogeology of the FdP playa lake can be found in Rodríguez-Rodríguez et al. (2016).

3 Methodology

3.1 Hydrological data compilation and water level calculation

We use hydrological information on the FdP playa lake from several sources (e.g. scientific reports from the Geological Survey of Spain and the Andalusian Autonomous Government) to elaborate on the hydrograph of the daily evolution of the water level in the playa lake. The water level above and below the lake floor was obtained from an automatic water level sensor installed in a piezometer placed inside the lake basin. Depth was expressed as altitude above sea level (m a.s.l.).

We reconstructed the palaeo water level of the FdP playa lake for comparison with lake sediments. To do that, we conducted water balances every 50 years over the last 35 kyr (700 water balances). We applied a lake water balance equation developed in previous studies of southern Iberian Peninsula playa lakes (e.g. Rodríguez-Rodríguez et al., 2015). The lake water balance considers average climatic conditions and is expressed as

$$\Delta V = P - E + S_{\mathrm{i}} - S_{\mathrm{o}} + \mathrm{GD} - \mathrm{GR}, \quad (1)$$

where ΔV (mm) is the change in the lake water level whose bathymetry is completely flat at 410 m a.s.l., P (mm) stands for precipitation onto the lake surface and E (mm) is the direct evaporation from the flooded surface. S_{i} stands for the surface runoff, which is calculated by means of a soil water balance. S_{o} is the surface outflow that, in the case of the FdP playa lake, is set to 0. GD represents the groundwater discharge from the regional aquifer to the lake and GR is the groundwater recharge from the lake to the aquifer. We assume that $S_{\mathrm{i}} + \mathrm{GD} - \mathrm{GR}$ equals BD (basin discharge), i.e. the total volume of the water runoff, surface water and groundwater flowing into the playa lake from the watershed. In the case of the FdP playa lake, previous studies suggest that the limit of the surface watershed coincides with that of the groundwater watershed (e.g. Linares, 1990), so BD can be calculated easily. Consequently, Eq. (1) is simplified to

$$\Delta V = P - E + \mathrm{BD}. \quad (2)$$

Mean precipitation data (mm yr^{-1}) were obtained from the sedimentary record of the Padul peatland (see Fig. 1b for the location) about 80 km from the FdP playa lake to E, which is based on fossil pollen data (Camuera et al., 2022). There are no climatic differences between the locations. We filled data gaps by interpolation using linear regression between available data (Fig. 4). Atmospheric temperature data from 0 to 15 kyr BP were obtained from sea surface temperature (SST) reconstructions in the Alborán Sea by Català et al. (2019) and Morcillo-Montalbá et al. (2021) from 15 to 35 kyr BP. We made the correlation between the Cabo de Gata buoy (comparable to SST) and the weather station close to the FdP playa lake (Antequera weather station), and we obtained a meaningful correlation coefficient of 0.76. Consequently, we assume that the long-term air temperature in the surroundings of the FdP playa lake ($\sim$ 50 km from the seashore) varied in the same fashion and magnitude as the SST. We used the palaeo temperature record to calculate potential evapotranspiration (PET) with the Thornthwaite method, using TRASERO software for the analysis and calculation of hydrological time series (Rodríguez-Hernández et al., 2007). We corrected these values by multiplying by 1.15 because this method usually underestimates real evapotranspiration (e.g. Rodríguez-Rodríguez et al., 2016). We obtained monthly potential E values that were later converted

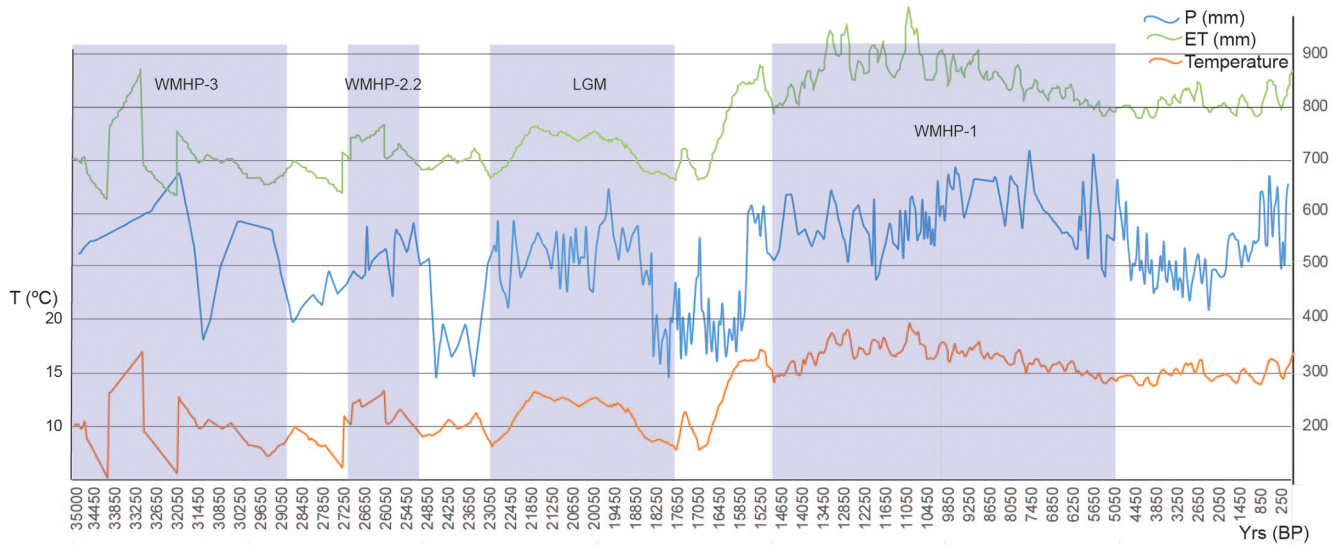

Figure 4. Temperature, ET and precipitation reconstruction during the past 35 kyr in the southern Iberian Peninsula (Català et al., 2019; Morcillo-Montalbá et al., 2021; Camuera et al., 2022) and the FdP water level oscillation according to Höbig et al. (2016).

to annual potential E values. BD, obtained from the soil water balance, was calculated with the same software using monthly potential E and the water-holding capacity (WHC) (Rodríguez-Hernandéz et al., 2007). The WHC is the amount of water a soil can hold without generating runoff, and it depends on the soil texture. We considered that water inputs only come from the watershed, which is assumed to have remained constant over the past 35 kyr. We ran the calculations (Allen et al., 2011) using two values of the WHC, 50 and 75 mm, to create two series of the maximum lake level. We have applied low-permeability values according to the rocks cropping out in the FdP watershed. We converted monthly water surplus to yearly surplus and then multiplied this value by the FdP watershed / average flooded area relationship (W/AFS) to obtain the amount of yearly BD (mm). BD includes the groundwater coming from the karstic aquifers and the surface runoff coming from the whole of the FdP playa-lake watershed. We assume that, when the water level is between 0 and 2 m, the AFS remains constant, so that the W/AFS relationship does not change (Rodríguez-Rodríguez et al., 2016). Then, we obtained the increase in the lake level (ΔV) every 50 years. Considering the FdP playa lake's behaviour from 1983 to 2012, we also assume that the FdP water level must start at 0 mm every year in most cases, and then ΔV equals the lake level. Importantly, to obtain the maximum water level, we must sum ΔV to the water level at the end of the previous hydrological year during wet years. We cannot make calculations for every year because the step of our palaeoclimate series is 50 years (Fig. 4). Hence, we chose the most humid period ($P = 700$ mm, $\mathrm{ET_o} = 850$ mm and runoff $= 75$ mm; Fig. 4) and performed iterative calculations per year for 50 years, keeping the climate conditions the same but changing the W/AFS relationship. Thus, we recalculated the AFS for every year, depending on the water level reached in the previous year.

3.2 Geomorphological and structural data

We improved the previous cartography of the FdP playa-lake sediments by focusing on the recent erosive and depositional landforms. Using slope maps, ortho-images and a 1 : 10 000 digital elevation model, we created an accurate cartography of playa-lake sediments associated with the FdP playa lake. We also constrained the Pliocene-to-Pleistocene landforms (Fig. 3). We collected structural data from those structures that affect Pliocene or younger sediments, whose scale ranges from several hundred metres to the kilometre scale (Fig. 3).

3.3 Compilation of geochronological and sedimentological data of the FdP sediments

We combined previously published geochronological data on FdP sediments to create a chronological framework for the lake evolution and discuss the reliability of the current age model. In this regard, Höbig et al. (2016) obtained 17 accelerator mass spectrometry (AMS) radiocarbon ages conducted on bulk sediment, pollen, charcoal and remains of plants and seeds from the 14 m sediment core 2013-04 recovered from the southern margin of the lake (Table 1, Fig. 5). In addition, we used eight recent U–Th ages obtained from gypsum crystals of core 2012-PL1 (1.4 m long) collected from the central part of the basin (Obert et al., 2022). Radiocarbon dates were calibrated into calendar years using the IntCal 13 curve (Reimer et al., 2020). A Bayesian age–depth model was calculated using the Rbacon R package (version 2.5 – March 2023; Blaauw and Christen, 2011) (Fig. 5).

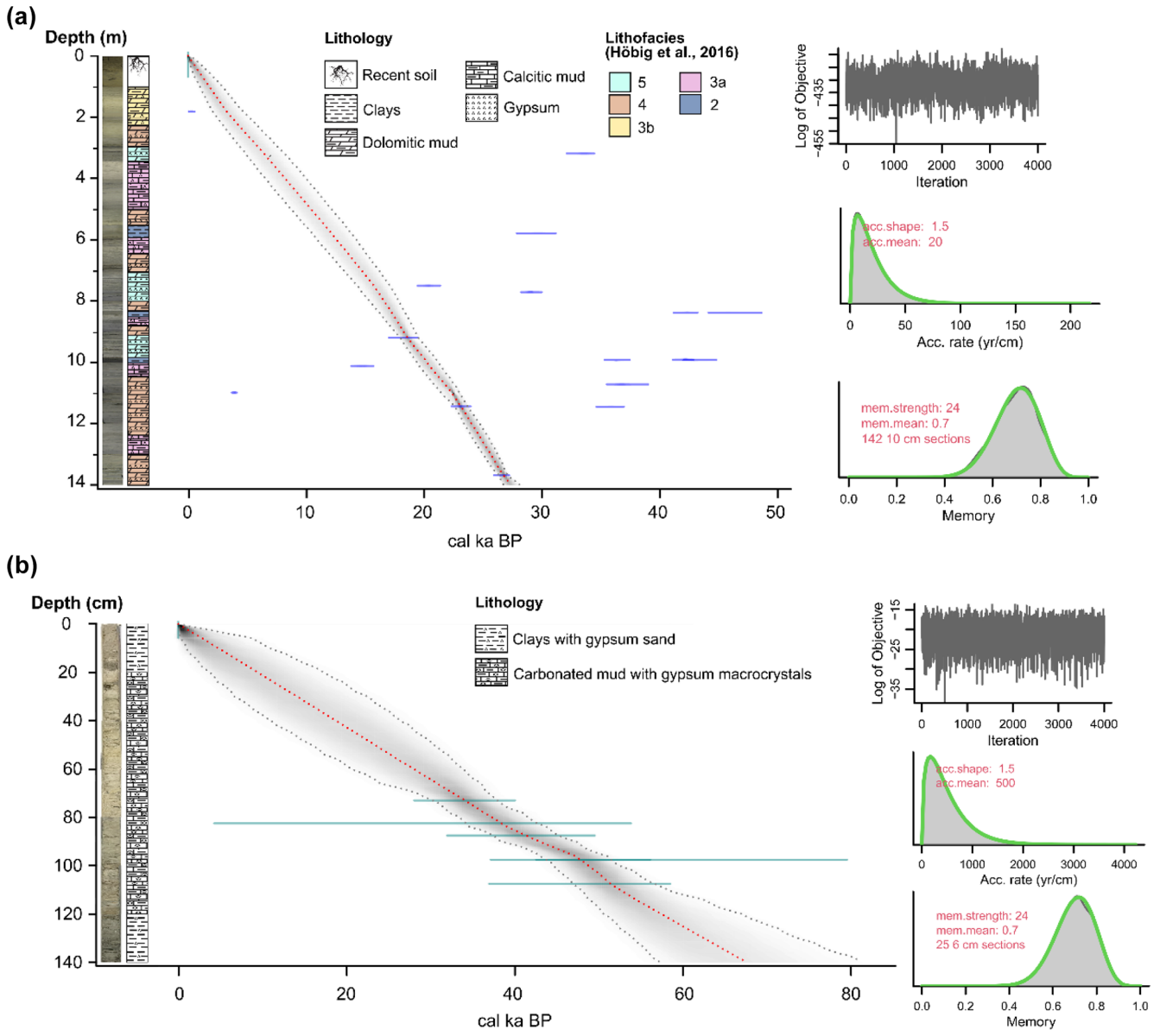

Figure 5. **(a)** Sedimentary sequence, lithology, lithofacies interpreted by Höbig et al. (2016) and age–depth model with a 95 % confidence range (grey shade) and the single best model (red median line) of core 2013-04. The calibrated ^{14}C dates are presented together with their uncertainty in blue. The iteration plot shows a rather stationary distribution. The prior and posterior distributions of the accumulation rate are depicted in the accumulation rate plot as the green and grey lines, respectively. The prior and posterior model memory distributions are shown as the green and grey lines, respectively, in the memory plot. **(b)** Sedimentary sequence, lithology and age–depth model (95 % confidence interval and red median line) of core 2012-PL1. For the age model references, see Table 1.

We investigate in detail the sedimentology of cores 2013-04 and 2012-PL1, which mostly comprises laminated clayey and carbonated sediments as well as different types of gypsum deposits ranging from gypsum sand to several prismatic selenite crystals 1 cm long. We primarily focus on the morphology of the gypsum crystals to evaluate either the primary or diagenetic origins of gypsum at various depths and use the criteria of Cody and Cody (1988) to identify different depositional environments between the FdP playa lake's sediments' southern margin and their central part.

4 Results

4.1 Geology of the FdP watershed

In this section, we describe the morphology of sedimentary bodies originating during the FdP playa-lake development

Table 1. Chronological data from the FdP playa lake's cores 2013-04 and 2012-PL1 (Höbig et al., 2016; Obert et al., 2022; see the locations in Fig. 3). Conventional radiocarbon ages from Höbig et al. (2016) were re-calibrated using the IntCal 20 curve (Reimer et al., 2020). In core 2012-PL1, "dc" refers to the activity ratios corrected with the conventional approach (Obert et al., 2022).

Core	Location	Sample ID	Depth (m)	Material	Conventional age (yr BP)	Calibrated age (yr BP)	2σ (cal yr BP)
2013-04	South-western lake shore	Beta-366926	7.71–7.72	Bulk sediment	24 810 ± 150	29 022	29 252 to 28 724
2013-04	South-western lake shore	Beta-365743	8.38–8.39	Bulk sediment	38 170 ± 420	42 327	42 675 to 41 983
2013-04	South-western lake shore	Beta-365744	9.93–9.94	Bulk sediment	39 690 ± 500	43 015	43 998 to 42 481
2013-04	South-western lake shore	Beta-365745	10.72–10.73	Bulk sediment	32 450 ± 240	36 761	37 360 to 36 244
2013-04	South-western lake shore	Beta-365746	11.45–11.46	Bulk sediment	31 450 ± 220	35 811	36 226 to 35 355
2013-04	South-western lake shore	Beta-365747	13.69–13.70	Bulk sediment	22 290 ± 100	26 673	26 964 to 26 335
2013-04	South-western lake shore	Beta-386843	9.91–9.93	Oogonia + seeds	37 750 ± 360	42 173	42 469 to 41 825
2013-04	South-western lake shore	Beta-386844	10.99–11.00	Charcoal	3570 ± 30	3,87	3907 to 3831
2013-04	South-western lake shore	COL2742.1.1	1.82–1.83	Plant/wood	212 ± 53	190	232 to 125
2013-04	South-western lake shore	COL2740.0.1	3.19–3.20	Pollen	29 053 ± 154	33 583	34 067 to 33 132
2013-04	South-western lake shore	COL2737.0.1	5.79–5.80	Pollen	25 464 ± 345	29 686	30 372 to 28 975
2013-04	South-western lake shore	COL2735.0.1	7.50–7.52	Pollen	16 825 ± 163	20 326	20 755 to 19 907
2013-04	South-western lake shore	COL2734.0.1	8.38–8.40	Pollen	43 510 ± 515	45 852	46 921 to 44 869
2013-04	South-western lake shore	COL2733.0.1	9.20–9.22	Pollen	15 008 ± 226	18 334	18 817 to 17 780
2013-04	South-western lake shore	COL2731.0.1	9.93–9.96	Pollen	31 999 ± 190	36 336	36 837 to 35 986
2013-04	South-western lake shore	COL2730.0.1	10.12–10.14	Pollen	12 491 ± 123	14 671	15 150 to 14 172
2013-04	South-western lake shore	COL2729.0.1	11.44–11.45	Pollen	19 159 ± 173	23 121	23 435 to 22 636
Core	Location	Sample ID	Depth (m)	Material	^{230}Th–U ages	^{230}Th–U ages^{dc}	
2012-PL1	Lake centre	LFP-1	0.73	Gypsum aggregates	40 400 ± 1500	34 000 ± 1500	
2012-PL1	Lake centre	LFP-2	0.825	Gypsum aggregates	37 700 ± 6700	29 000 ± 6200	
2012-PL1	Lake centre	LFP-3	0.875	Gypsum aggregates	49 700 ± 2300	40 700 ± 2200	
2012-PL1	Lake centre	LFP-4a	0.975	Gypsum aggregates	70 500 ± 5600	58 300 ± 5300	
2012-PL1	Lake centre	LFP-4b	0.975	Gypsum aggregates	58 700 ± 1600	49 300 ± 1700	
2012-PL1	Lake centre	LFP-5	1.075	Gypsum aggregates	66 200 ± 1700	47 700 ± 2700	
2012-PL1	Lake centre	LFP-6	1.325	Gypsum aggregates	113 600 ± 5900	76 000 ± 30 000	
2012-PL1	Lake centre	LFP-7	1.395	Gypsum aggregates	113 700 ± 4000	78 000 ± 30 000	

(Pleistocene to Holocene) and the recent structures that have been active at least during the last 2 Myr and may influence the FdP watershed and its flooded area.

4.1.1 Geomorphology of Pleistocene-to-Holocene sedimentary bodies

We differentiate sediments from two young depositional environments: fine-grained partly evaporitic, lacustrine deposits related to the FdP playa lake and colluvial Pleistocene and Holocene pediments.

Lacustrine sediments related to the current FdP playa lake crop out quasi-horizontally at 410 m a.s.l. (lake base level, LBL) and extend to the north-east, outside the playa lake's current area, where they reach altitudes of 425 m a.s.l. (Fig. 3). Here, they show a smooth slope (from 1 % to 1.5 %) towards the south-west (Fig. 3b). Towards the east, lacustrine deposits of the La Nava playa lake are currently isolated from the FdP playa-lake sediments by a topographic high. Here, they are horizontal and are located 3 m above the FdP LBL (respective altitudes of 413 m and 410 m; Fig. 3a and e).

The FdP watershed presents both depositional and erosive pediments. They are characterised by red soils, sometimes called "red rendzinas", "terra rossa" or chromic Luvisols, that developed over Miocene limestones, which are very abundant in the Mediterranean (Sandler et al., 2015). Occasionally, these soils also include carbonate crusts, so-called "calcretes", which typically form in Mediterranean climates (Alonso-Zarza and Wright, 2010). The most intensive development of such red Mediterranean soils occurred from the Miocene to the Late Pleistocene due to the numerous climate fluctuations in those periods (Atalai, 2020). Pleistocene ages seem to be consistent with our observations, as red soils overlie Pliocene-to-Pleistocene conglomerates and sandstones and are covered by Holocene lacustrine deposits (Fig. 3a). Their thickness varies from 0 to 0.5 m in the case of erosive pediments, while they reach more than 1 m in the case of colluvial pediments (glacis deposits). They all constitute flat surfaces that are 3d). The best-preserved one is located west of the FdP playa-lake sediments at about 470 m a.s.l. (Fig. 3c). It is related to an erosive pediment that truncates Tortonian-to-Messinian calcarenite beds (Fig. 3c) and extends over 1000 hm^2. Headwaters from both Atlantic rivers and FdP streams are eroding this thin red soil (Fig. 3a). The thickest depositional pediments are found in depressed areas (at ca. 420 m a.s.l.) close to the current FdP LBL (Fig. 3a). The red rendzinas soils in these deposits have a complete soil profile.

4.1.2 Tectonic structures and kinematics

The structures involving Tortonian-to-Holocene sediments are faults that can be grouped into three sets.

The NE–SW-striking La Nava fault zone, related to the western branch of the HTZ, affects Tortonian-to-Messinian sediments south-east of the FdP playa-lake sediments (Fig. 3a and f). This fault is ca. 10 km long and extends south of the Campillos playa-lake system. Fault surfaces strike N20–45° E and dip between 70 and 90° WNW. Slickenlines show pitches up to 15° SSW (Fig. 3f). This, combined with kinematic indicators such as S–C-like structures and calcite and gypsum slickenfibres, indicates a dominant left-lateral strike–slip movement and a subordinate normal movement throwing the western block down (Fig. 3a and f). Other highly dipping NE–SW faults affect Jurassic and Pliocene outcrops to the west of the FdP playa lake's sediments (Fig. 3a).

WNW–ESE- to NW–SE-trending right-lateral faults constitute the 10 km Las Latas fault zone that coincides with the southern water divide of the FdP watershed. Fault surfaces strike 60–85° E and dip 65–90° NNE. Slickenlines show pitches of up to 35° ESE. Kinematic indicators such as S–C-like structures indicate a dominant right-lateral strike–slip movement with a subordinate normal component, which lowers the northern block where the FdP watershed is located (Fig. 3a). We interpret this fault zone as a synthetic Riedel fault of the ABSZ (Figs. 2 and 3a). Other WNW–ESE faults are found on the western margin of the FdP watershed (Fig. 3a).

The western water divide of the FdP watershed coincides with the hinge zone of a kilometre-scale anti-form, deforming Tortonian-to-Messinian units. Its axis plunges 25° towards the south-west and its hinge zone is locally truncated by a Pleistocene erosive pediment (Fig. 3a and c).

4.2 Chronological framework and description of sedimentary facies

The radiocarbon dates of the sediments in core 2013-04, from the southern margin of the lake, range from 0.8 to 45 kyr BP (Table 1) (Höbig et al., 2016). They show large dispersion and age reversals, especially in the lower section, which may be due to reworking of older sediments in the basin up to 45 kyr old, as suggested by the oldest obtained ages (Fig. 5). Nevertheless, the relatively low Gelman and Rubin reduction factor (< 1.05), the convergence test and the stable log-posterior time series suggest a relatively reliable age model and good fitting (Fig. 5a). According to this model, the sedimentation rate in core 2013-04 comprises the last 26.4 cal kyr BP. For core 2012-PL1, the available ages only correspond to the deeper and central section of the 1.4 m core (0.73 to 1.39 m; Table 1), and the analytical errors of the ages are up to 50 % in some cases (LFP-6 and LFP-7, excluded in the model), so the ages must be regarded with caution. The age of gypsum crystals in the sediment provided by Obert et al. (2022) ranges from 34 ± 1.5 to 47 ± 2.7 cal kyr BP, with no age reversals considering the large analytical errors of some ages. The chronological model for core 2012-PL1 suggests that the deepest core section is at least 40–50 kyr old (Fig. 5b).

The sediments in core 2013-04 (Fig. 6a) are essentially composed of fine-grained materials, primarily clays and carbonate (calcitic, aragonitic or dolomitic) muds, along with evaporites represented by gypsum and halite. Gypsum shows several crystal morphologies, including single or twinned micro- and macro-lenticular crystals (which often developed interstitially in the clay or mud), millimetre- to centimetre-scale prismatic crystals and subangular to rounded gypsum sand grains, interpreted previously by Höbig et al. (2016) as "detrital" gypsum (Fig. 6). These authors also assessed different lithofacies in core 2013-04 based on macroscopic and microscopic observation and geochemical data (Fig. 6a). Lithofacies 2 contains layers of 1 cm massive clays with micro-crystals of lenticular gypsum, while lithofacies 3a and 3b are mainly formed by beds of carbonate mud with micro-lenticular gypsum crystals that sometimes are embedded in the mud. In turn, 1 cm layers of dolomitic mud and gypsum sand grains, both with interstitial 1 mm lenticular gypsum crystals, are the principal components of lithofacies 4 and 5 and are only differentiated by the abundance of gypsum sand layers that are more frequent in lithofacies 5. Less abundant are prismatic crystals and 1 cm macro-crystals of lenticular gypsum.

In core 2012-PL1, the upper 20 cm are dominated by laminated grey clays intercalated with 1 mm layers of gypsum sand. Between 20 and 120 cm, the core is composed of pale carbonate mud with embedded prismatic gypsum macro-crystals at the centimetre scale (Fig. 6). The deepest section shows a similar composition to the top, but the clays have a darker grey colour.

4.3 FdP hydrology

4.3.1 Pleistocene-to-Holocene water level evolution of the FdP playa lake

The results of the hydrological modelling of the FdP playa lake over the past 35 kyr are shown in Fig. 7. This includes modelling using WHCs of 75 and 50 mm. For these calculations, first we ensured that both the FdP watershed (W) and AFS remained constant. When using a WHC of 75 mm, the modelled runoff for the FdP watershed during the entire period is relatively low (Fig. 7a). Consequently, the lake was probably dry for most of the time, and increases in the water level (ΔV) did not reach 0.5 m, except for a humid period from 32 to 30 kyr BP (Fig. 7a). We consider this model to be unrealistic because, with similar precipitation and evapotranspiration values (350–700 mm for P and close to 1000 mm for PET) in the historical period from 1983 to 2022, much

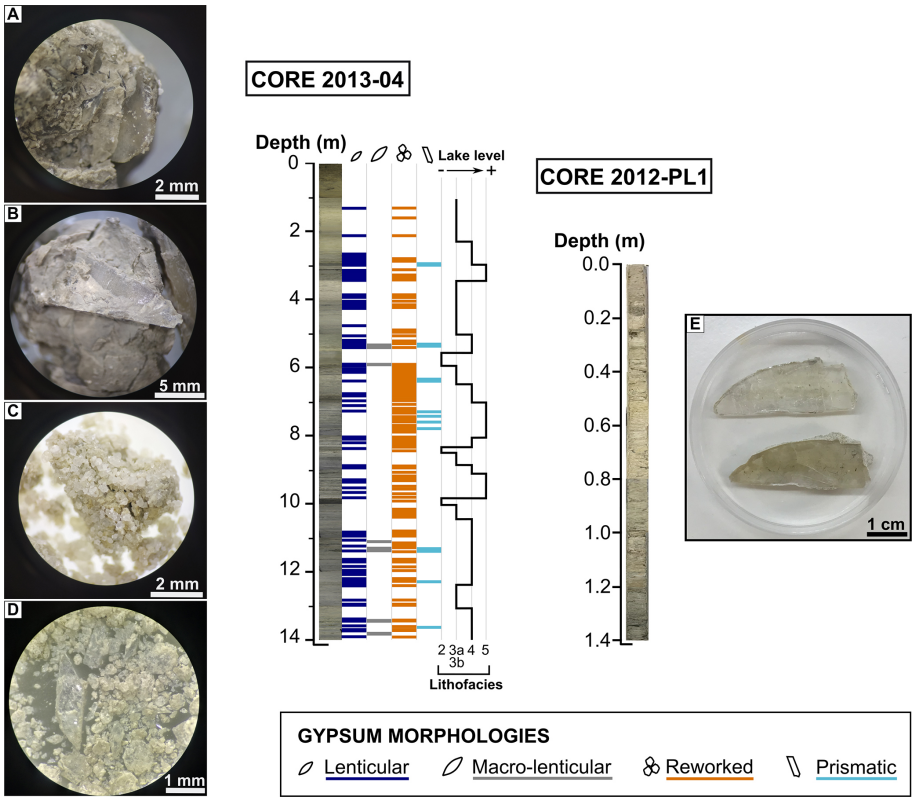

Figure 6. Distribution of the gypsum morphologies in cores 2013-04 and 2012-PL1. **(a)** Lenticular crystals. **(b)** Macro-lenticular crystals. **(c)** Rounded sand-sized gypsum grains (reworked). **(d)** Prismatic crystals. **(e)** Prismatic macro-crystals. The FdP playa-lake level reconstruction by Höbig et al. (2016) based on sedimentary facies is shown for comparison.

higher runoff values were observed (Rodríguez-Rodríguez et al., 2016; Fig. 7). Consequently, a WHC of 75 mm was discarded for additional analyses. When using a WHC of 50 mm, runoff values in the FdP watershed during some periods are like present values (ca. 10 %–15 % of precipitation). However, the increase in the lake level (ΔV) is always below 2 m (Fig. 7b). Maximum values were obtained between 32 and 30 kyr, when the ΔV was up to 1.8 m, and between 10 and 4 kyr, with values ranging from 0.5 to 1.8 m (Fig. 6b). ΔV during the last 1000 years ranged from 0.5 to 1 m, which is equal to the current ΔV FdP playa lake (Figs. 7 and 8).

The FdP playa lake probably behaved as a seasonal lake, in which case ΔV would be equal to the maximum water level. However, during rainy periods, it probably behaved as a permanent lake. In this case, to obtain the maximum water lake level, we recalculated the AFS for every year during extremely rainy periods of 50 years ($P = 700$ mm, PET = 850 mm and runoff = 75 mm; Fig. 7b), depending on the water level reached in the previous year (Fig. 9). We found that the FdP water level never surpassed a height of 5 m over the lake bed. Because of the flat bathymetry of the FdP playa lake, the W/AFS relationship used to calculate the BD decreases from 11.1 to ca. 3 (i.e. the W area was triple the size of the AFS area) when the FdP water level increases from 1 to 5 m (Fig. 10). Consequently, the water level stabilises at ca. 5 m, where water inputs are equal to water outputs (Fig. 9). This lake level could be reached before 14 years in the case of groundwater level increases. Given that there is no clear maximum water level, Fig. 10 shows the FdP flooded area from 1 to 6 m above the lake bed. The contour of the lake deposit outcrops is also indicated.

Several piezometers are installed at different depths to investigate the behaviour of the hyper-saline groundwater brine below the playa-lake floor (Fig. 11). The distribution of electrical conductivity values of water in the studied profiles remained relatively constant during the study period (1993–1998) in the different piezometers. The measurements in piezometers 2 and 3 reveal a transition zone ca. 1–2 m thick between the local rainwater and runoff from the catchment, which remains in the upper level because of its lower density, and brine beneath the FdP playa lake (Fig. 11). This transition zone is a result of mechanical dispersion and molecular diffusion processes. The theoretical Ghyben–Herzberg interface is located within the transition zone, and it remains there for 100 years once a playa lake dries up. Meanwhile, in piezometer 4, the southernmost piezometer, the interface is not so clear (Fig. 11).

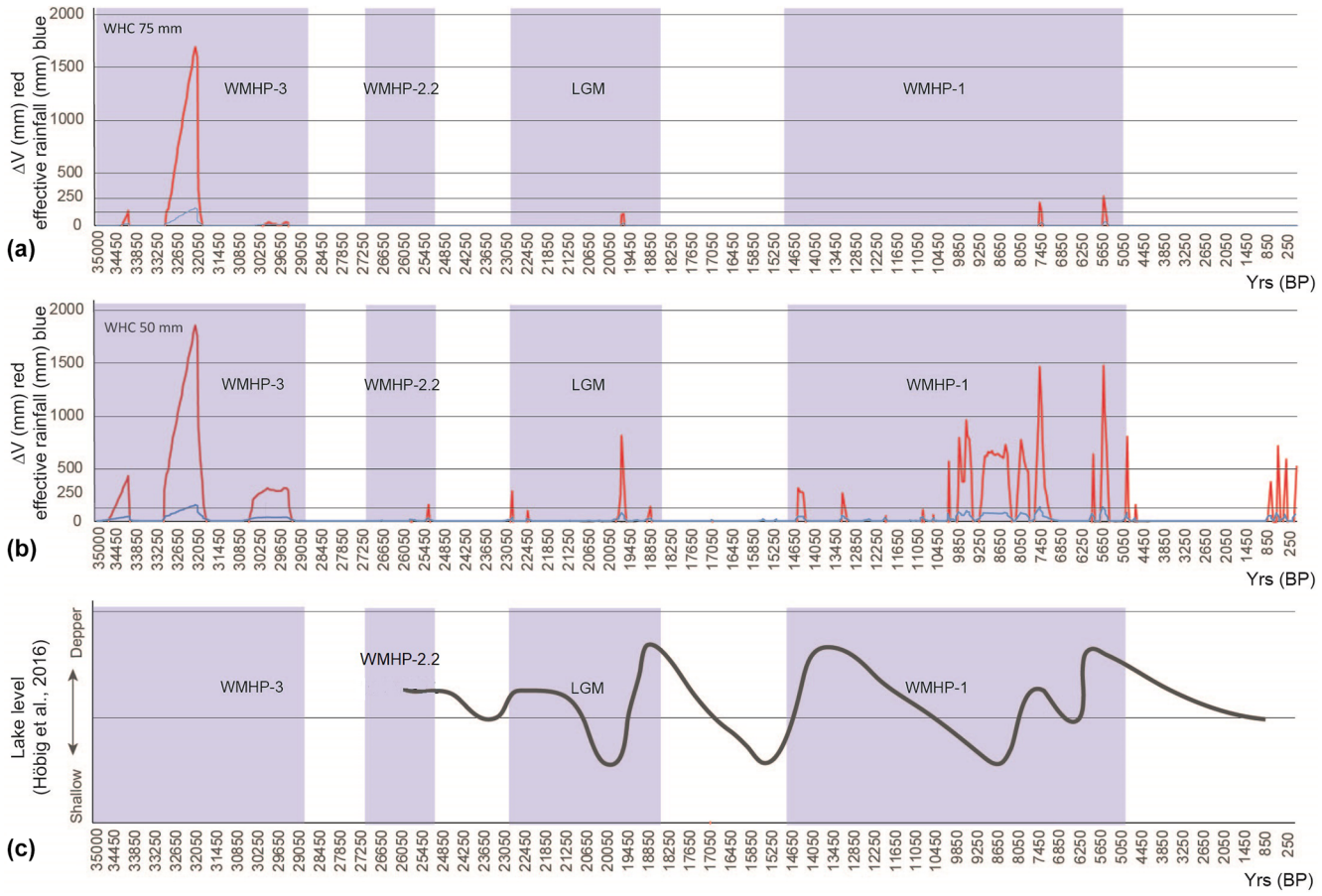

Figure 7. Model results showing ΔV in the FdP playa lake (in red) and effective rainfall (in blue) using WHCs of 75 mm **(a)** and 50 mm **(b)**. **(c)** Variations in the FdP lake level according to Höbig et al. (2016).

5 Discussion

5.1 The FdP evolution through its sedimentary record

Previous works based on radiocarbon dates suggested that the FdP playa lake is the oldest one investigated in the area. The earliest ages are ca. 26 kyr in the southern sector (Höbig et al., 2016) and may be earlier than ca. 50 kyr in the central basin, as suggested by recent chronological analyses of gypsum (Obert et al., 2022). Moreover, drills did not reach the contact between the lacustrine sediments and the basement (Triassic rocks), so the FdP inception was probably even earlier.

In our work, the gypsum deposits observed in the core from the south-western shore of the FdP playa lake (2013-04; Figs. 3a, 4a and 12) differ greatly from those observed in the core taken from its centre (2021-PL1; Figs. 3a, 4b and 12). The south-western gypsum deposits exhibit a wide range of crystal variations and sizes, with a majority of fine grains, while only selenite crystals larger than 1 cm interbedded with mud are found in the lake bed in its central part (Fig. 5). The morphology of gypsum crystals in sediments of continental environments can offer hints to understand their depositional setting (Cody and Cody, 1988). According to these authors, larger prismatic crystal growth is chiefly independent of temperature, and it develops in environments with relatively low concentrations of dissolved organic compounds. Also, larger gypsum crystals are expected to grow under relatively stable conditions. These stable conditions can be attributed to periods of water level highstands and a more permanent playa-lake level (e.g. from 10 to 7.5 kyr ago; Fig. 3). Despite the uncertainty in the ages obtained by Obert et al. (2022), and assuming that the results of their challenging U–Th measurements are correct, the age of the sediments in the central basin is older than 48 kyr but may be as old as 98 kyr according to the age uncertainties. Importantly, sediments about 0.7 m below the playa-lake floor in its central part are 34±1.5 kyr (2012-PL1; Figs. 3a and 4b). This chronological model suggests that either the sedimentation rate of the upper 0.7 m was considerably low (0.02 mm yr^{-1}) during the past 34 kyr or, instead, part of the sediments that were deposited in the central area of the FdP playa lake during the Holocene may have been eroded or dissolved more recently. The topographic and tectonic uplift of the north-

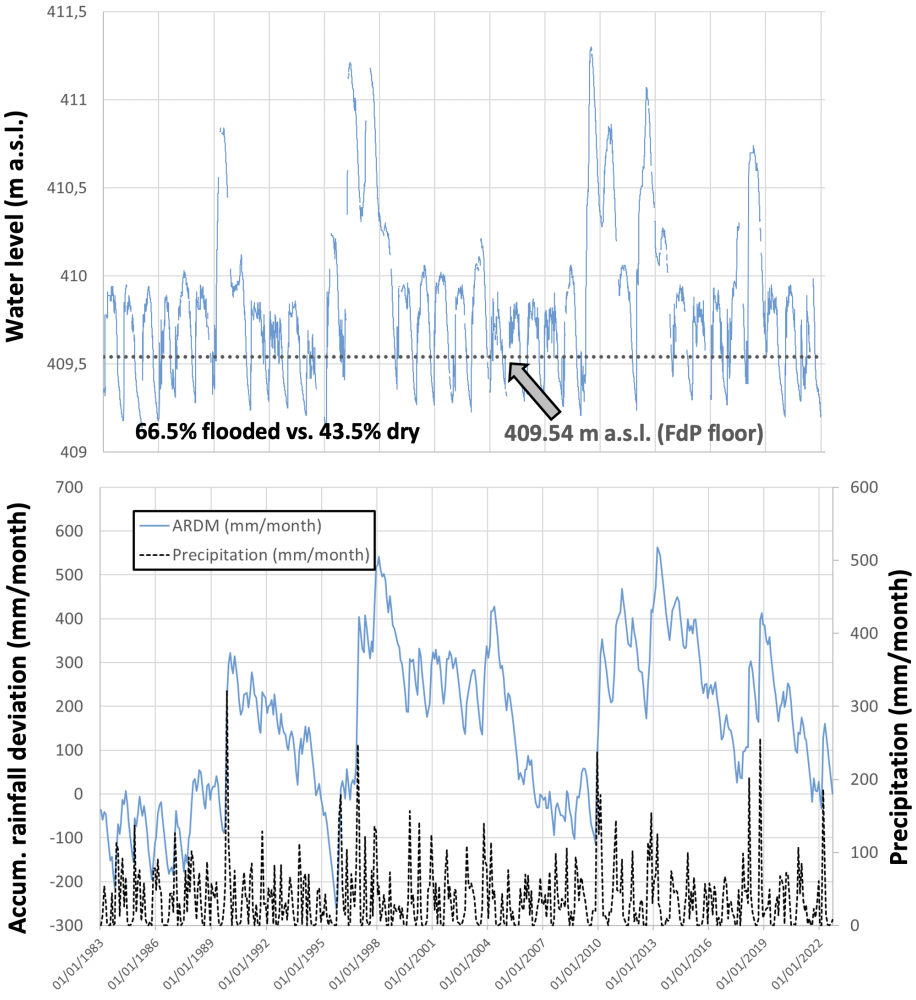

Figure 8. Variations in the FdP playa-lake water level from 1983 to 2022. These 4 decades include both dry and wet periods.

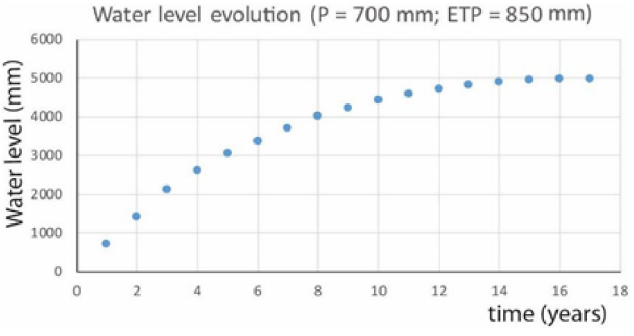

Figure 9. Results of the FdP water level assuming stable humid conditions during 17 years, when the water level stabilises at ca. 5 m above the lake bed.

ern part of the basin and the subsidence of its southern part may have favoured exposure of the northern sediments to erosion because of slow tilting of the basin to the south, which is congruent with the kinematics of its faulted boundaries (Fig. 12). Remobilisation of older lacustrine sediments because of waves produced by wind during highstand periods and/or by aeolian erosion during lowstand periods would have resulted in lake bed exposure and, consequently, migration of "reworked" gypsum grains to other parts of the basin. This agrees with the current slope shown by the lacustrine deposits in the north-eastern corner of the FdP playa-lake sediments, which reaches 1.5 % (Fig. 3b). Alternatively, we cannot rule out the possibility that the FdP playa lake split into some subbasins during its evolution. This could also explain the weak resemblance between 2012-PL1 and 2012-PL2 (Figs. 5 and 6).

Höbig et al. (2016) attributed the presence of rounded sand-sized gypsum grains found throughout the entire length of core 2013-04 from the south-western shore to periods when playa-lake water agitation caused sediment rework-

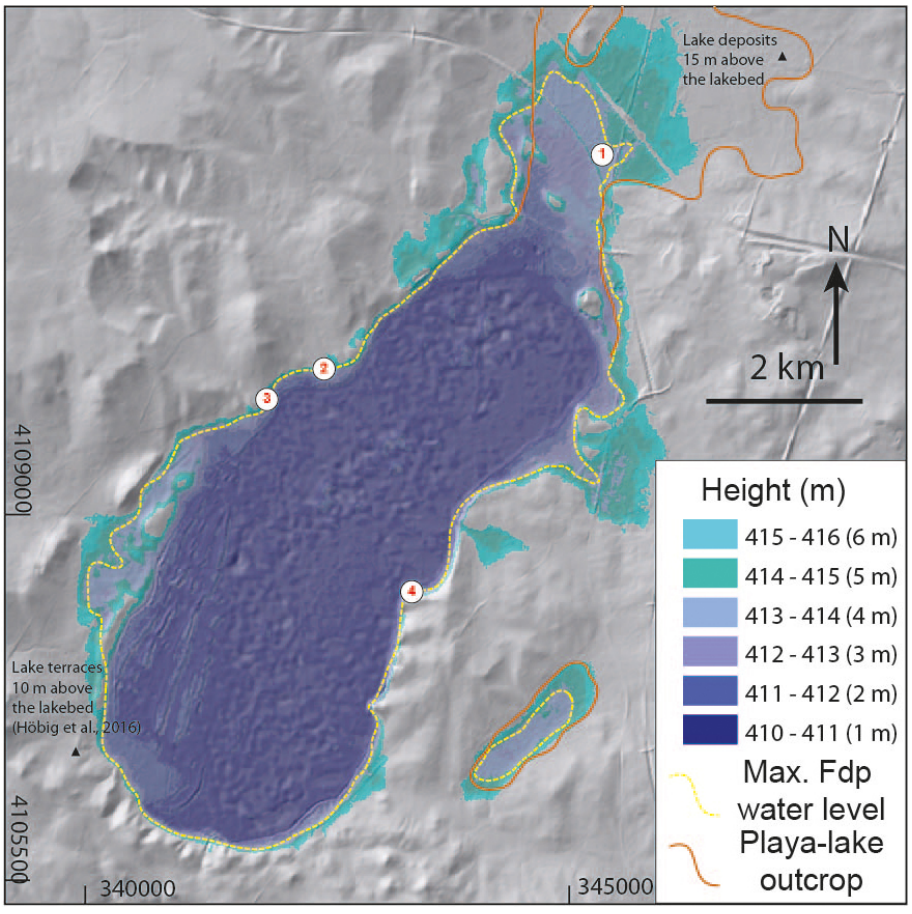

Figure 10. Simulation of the FdP playa lake's AFS if the water level reaches 1 to 6 m using the current topography. The boundary of the Pleistocene-to-Holocene FdP playa lake's sediments is also displayed (see Sect. 3.2 for the methodology). The locations of piezometers 1 to 4 are shown.

ing and transportation from shallower to deeper areas. This is consistent with the hypothesis of lacustrine basin migration towards the south-west as the elevation of the northern area could have produced a more energetic environment in the south-west (Fig. 12). In this scenario, sediments from the north-east may be continuously eroded, transported and deposited towards the south-west at different distances from the source area. Unfortunately, no scientific drilling reaching the contact between the lacustrine sediments and the underlying Triassic material has been conducted in the FdP playa lake to date, either on the margins or in the central part of the basin. Further investigations of the FdP sedimentary sequence may shed light on the geometry of this contact. According to our hypothesis, this contact may be in a deeper position in the southern playa-lake sector than in its northern part because of the southward tilting of the basin.

5.2 Factors controlling the FdP flooded area geometry and evolution

Here we propose a hydrological model for the FdP playa lake based on a water balance simplified to precipitation and surface and subsurface runoff from the watershed as water inputs and ET as water outputs (Rodríguez-Rodríguez et al., 2016). According to this model, the watershed area is in equilibrium with the FdP average flooding surface (i.e. it maintains a constant W/AFS ratio) under almost unchanging climate conditions (precipitation and temperatures that control the potential evapotranspiration). We considered that the endorheic watershed size has remained constant along the FdP playa lake's lifespan in the last 35 kyr. Although the watershed geometry could have changed, the FdP watershed area probably remained constant. Some plausible increases or decreases in the FdP watershed ($< 10\,\mathrm{km}^2$, 6 % of the current watershed) would not imply significant increases in the W/AFS relationship (Fig. 13).

Precipitation (P) and ET values have changed during the last 35 kyr in the southern Iberian Peninsula: P ranged from

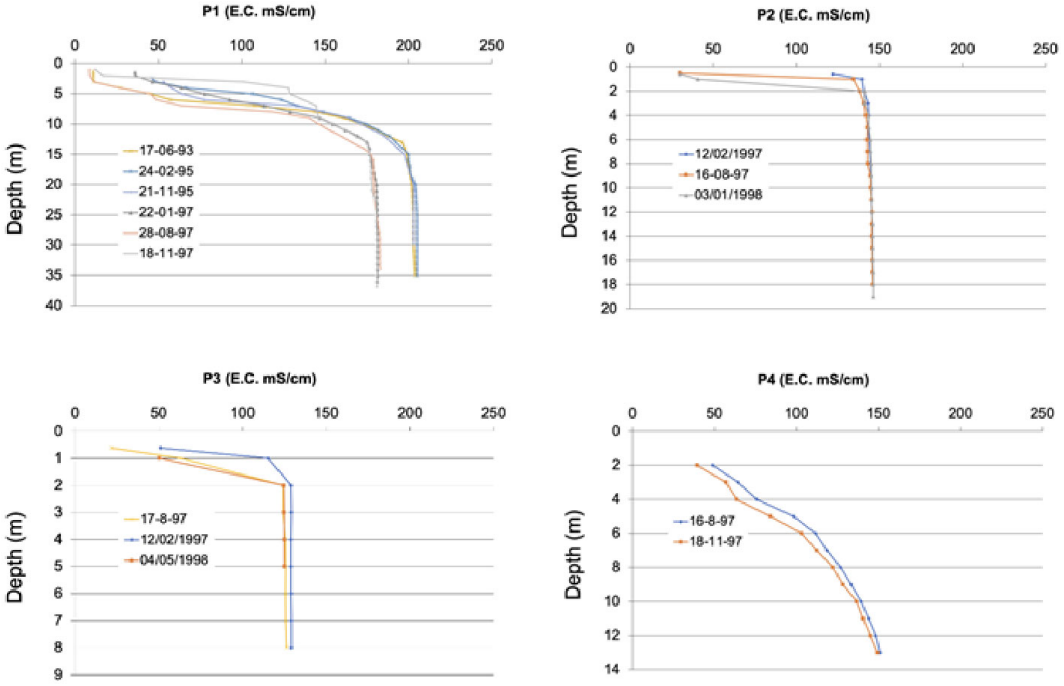

Figure 11. EC profiles of the groundwater in the piezometers shown in Fig. 10. Note that nowadays piezometer 1 is in an area outside the current playa-lake basin. Differences in EC between the 1993/1995 and 1997 profiles are attributed to differences in precipitation.

350 to 700 mm and ET varied between 650 and 1000 mm (Fig. 4). With these climatic conditions, the FdP playa lake has probably behaved like a discharge system since its inception. We chose the wettest period to calculate the highest expected water level (at ca. 6 kyr BP: $P = 700$ mm and ET = 820 mm; Fig. 6) and performed iterative calculations by changing the W/AFS relationship for 50 years (Fig. 9). Our calculations suggest that the maximum feasible lake water level under such climate conditions is 5 m. During some extremely wet periods described by Camuera et al. (2022), such as WMHP-3 (39–29 kyr BP), WMHP-2 (27–18.5 kyr BP; WMHP-2.2 at 27–25 kyr BP and WMHP-2.1 at 23–18.5 kyr) and WMHP-1 (15.5–5 kyr BP), the FdP playa lake probably increased its hydroperiod to more than 80 %. Indeed, it could have behaved as a permanent lake during short periods, as it currently occurs with other lakes in this area (e.g. Lake Amarga; Jiménez-Bonilla et al., 2023a, b). For these extremely wet periods, our model does not contemplate a possible water supply from the aquifer, which would reduce the time to reach the maximum water level (Fig. 9). However, the FdP water level probably never reached 5 m above the lake bed because of the variability of the Mediterranean climate conditions (dry periods alternating with wet periods). More than 10 humid years are needed to obtain this value (Fig. 9). Moreover, the lake level during the past 30 years has never exceeded 2 m (Fig. 8). As can be deduced from Fig. 8, the FdP playa lake has been dry almost every summer during the period with instrumental records (1983–2022), except for two humid periods (1996–1997 and 2010–2011) in which the it remained flooded for 2 consecutive years. From the analyses of the data record obtained in the deepest part of the playa lake's floor, during the daily record of the lake's hydroperiod, 9710 out of 14 610 d, the water level was higher than 409.54 m a.s.l., which is the altitude at which the level drops to 0 m (consequently, the playa lake dries out completely). So, the average flooded period (hydroperiod) for this playa lake, to date, is 66.5 % (see Fig. 8 for details). Comparing our lake level reconstruction with that of Höbig et al. (2016), based on the sediment sequence, we observe that the lake level is higher during the Last Glacial Maximum (LGM) and some late glacial periods but relatively lower during the Holocene for the Höbig et al. (2016) reconstruction (Fig. 7). This could be due to a recharge to the karstic aquifers during the winter. Then, most playa-lake sediments should have been deposited on the lake shores between 0 and 5 m above the lake bed. Nevertheless, Pleistocene-to-Holocene FdP playa lake's sediments are distributed from 0 m to more than 15 m above the lake bed north-east of the playa lake (Figs. 3a, b, 10 and 13). In this regard, previous works have interpreted some sandstone outcrops located to the south of the playa lake as being lacustrine terraces, which are currently 10 m above the lake bed due to climate changes (Höbig et al., 2016). However, these outcrops show features pointing to a high-energy environment between the continent and the ocean: angular clasts of a wide variety of sources and a calcareous cement (see the Pliocene

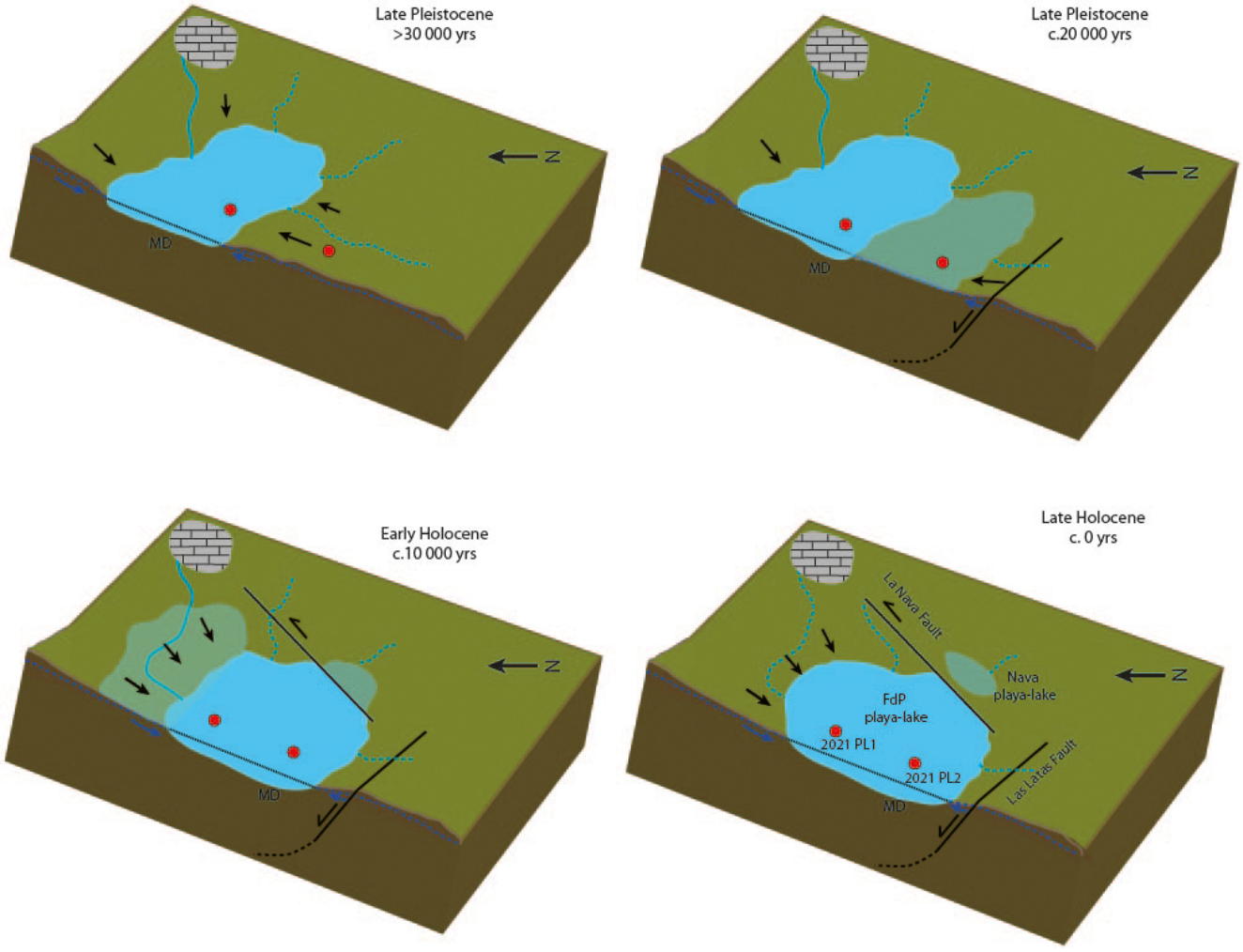

Figure 12. Schematic evolution of the FdP playa lake during the Late Pleistocene and Holocene showing the main active structures and the evolution of the flooded area according to neotectonics and variations in the climate. The black arrows show the main sediment supply. MD: main depocentre. The core locations are represented by the red dots.

conglomerates and sandstones in Fig. 3). These rocks are similar to other continental–marine transitional Pliocene deposits found within the ADZ (Cruz-Sanjulián, 1991; see the stars in Fig. 13). Moreover, these conglomerates and sandstones are made up of clasts from the Alborán domain, which is currently out of the FdP endorheic watershed. Then, these sediments were deposited before the FdP watershed's inception. We interpreted these sediments as being the playa-lake basement instead of FdP playa-lake sediments. In contrast, to the north-east of the current FdP playa lake, these deposits are dark soils with a flat topography which correspond to old lake deposits, as we showed in our results (Fig. 3).

The presence of playa-lake sediments more than 10 m above the lake bed to the north-east suggests a displacement of the FdP playa lake towards the south-west from the Late Pleistocene to the Holocene. Such behaviour is also consistent with the analyses of the electroconductivity (EC) profiles performed in the piezometers (Fig. 11). The development and formation of a sharp transition zone between the underlying groundwater brine and the upper brackish-to-fresh discharge are detected in the EC profile. As commented on before, this chemocline is associated with fluctuations in the water level of the playa lake due to both seasonal drying and the climatic cycles as well as variations in the piezometric level of the aquifer. The observations indicate the existence of a brine reflux from the playa-lake floor beneath the transition zone, like what has been studied in well-documented analogous playa lakes elsewhere (e.g. the Tyrrell Basin; Macumber, 1992) and also in this same system (Kohfahl et al., 2008).

The presence of a well-defined interface 1 to 5 m wide towards the north of the playa lake (piezometer 1; see Fig. 11), in an area where the FdP's current playa-lake floor is absent, could indicate a potential migration of the lacustrine basin

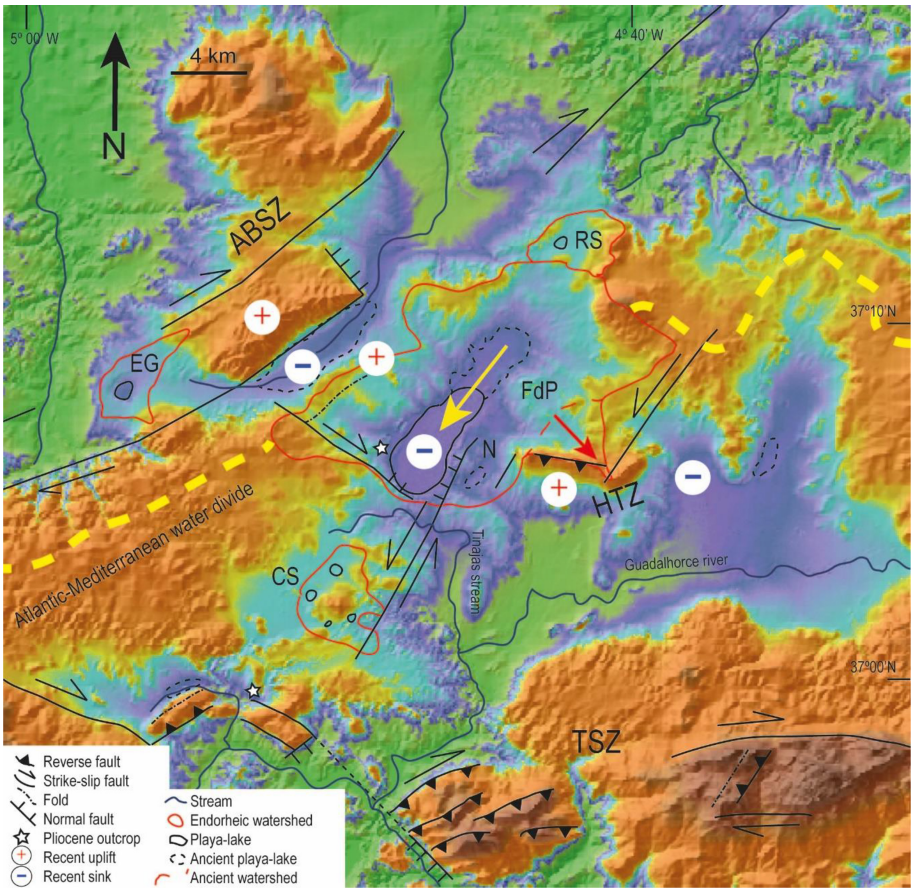

Figure 13. DEM of the ADZ, where the Atlantic–Mediterranean divide (in yellow) is located in this sector of the Betics and the FdP watershed develops. The main structures are shown together with their estimated recent movements. EG: El Gosque, FdP: Fuente de Piedra, CS: Campillos system, RS: Ratosa system and N. Stars: locations of the Pliocene conglomerates and sandstones.

from NNE to SSW. This hypothesis is supported by two observations:

1. The interface is highly stable over time; therefore, once formed, it would take a considerable amount of time for it to be washed away.

2. In piezometer 4, located further south, the interface is considerably weaker, suggesting that the playa-lake floor has not existed in this position for that long.

This finding supports the hypothesis of a lacustrine basin migration over time that was potentially caused by tectonic factors. Indeed, both the Las Latas and La Nava faults affect Pliocene sediments. The locations of the earthquakes and focal mechanisms are compatible with their kinematics (Jiménez-Bonilla et al., 2024). Consequently, both faults were probably active during the Quaternary. Moreover, the south-westerly movement of the FdP playa lake is consistent with the kinematics of recent faults which determine its boundaries (Fig. 13; Jiménez-Bonilla et al., 2023a, b). Thus, the left-lateral component of the La Nava fault would have induced the south-westerly displacement of the main FdP depocentre. Additionally, the relative uplift of the northeastern edge of the FdP playa lake is compatible with its southward tilting hanging wall associated with the downthrowing of the Las Latas fault. According to this, the normal dip–slip component of both the La Nava and Las Latas faults would have produced the FdP relative sinking of the FdP playa lake, preventing its siltation and capture by Mediterranean streams (e.g. the Tinajas stream; Fig. 13). Therefore, the long lifespan of the FdP playa lake (> 30 kyr), which is unusual for playa lakes in southern Spain (compared with, for example, the 11 kyr-old Ballestera playa lake; García-Alix et al., 2022), would have been favoured by the tectonic activity in this area. It is likely that the relict La Nava playa lake (Figs. 3a, e and 13) was formerly part of the FdP playa lake and was subsequently separated by uplift of the La Nava fault footwall. Consequently, the La Nava playa lake is currently a recharge system linked to the FdP playa lake. In summary, the FdP playa-lake geometry and evolution seem to have been influenced, since the beginning, by the recent active tectonic activity in the area, governed by the transpressive kinematics of the TSZ and ABSZ. This tectonic scenery would

be responsible for the NW–SE relief segmentation that generated the Antequera Depression Area (ADA), favouring the inception of several endorheic basins there. Focusing on the FdP playa lake, and according to our results (Fig. 5), its inception occurred at least 50 kyr ago, with its further evolution controlled by faults linked to the transpressive kinematics. In this regard, focal mechanisms of earthquakes and geomorphological studies support the current activity of both shear zones (Jiménez-Bonilla et al., 2015, 2023b). Consequently, active tectonics seem to be the key factors in the shaping of these wetlands within this Betics fold-and-thrust belt segment.

6 Conclusions

Previous studies attributed the presence of lacustrine deposits surrounding the Fuente de Piedra playa lake to climate fluctuation (Höbig et al., 2016). In this work, we applied hydrological modelling for the Fuente de Piedra (FdP) playa lake during its lifespan (> 35 kyr). To this end, we reconstructed direct evaporation, ET and runoff from previously published P and temperature, and we calculated the increase in the water level from the playa-lake bottom every 50 years. The increase in the water level never reached 2 m, and iterative calculations show that the maximum water level is lower than 5 m. However, we detected lacustrine deposits more than 10 m above the lake bed, and then additional forces other than climate changes were evaluated here. According to the geological results, we propose south-westerly displacement of the FdP playa lake during the Pleistocene and Holocene because of recent tectonic activity. This displacement is supported by the activity of the left-lateral-dominated La Nava fault and the dip–slip-dominated Las Latas fault, which contribute to the downthrowing and tilting of the block where the FdP playa lake is located. Other lines of evidence support this hypothesis:

1. There are lacustrine sediments related to the current FdP playa lake more than 15 m above the lake bed in the north-eastern corner of the playa lake. To the east of the FdP playa lake an isolated lacustrine deposit is located 3 m above the present FdP lake bed. The uplift and isolation of the patch are compatible with the La Nava fault kinematics.

2. The presence of a well-defined water interface towards the north of the FdP watershed, above the maximum FdP water level, also indicates a south-westerly migration of the FdP depocentre.

3. The morphologies of gypsum found in the sediments indicate the existence of primary gypsum formed in situ during certain periods. Significant amounts of reworked gypsum, probably transported from the northern parts of the basin, were also deposited throughout most of the time covered by this sedimentary sequence, especially to the south. The south-westerly tilting of the playa lake may have facilitated this process.

Our study confirms the importance of multidisciplinary investigations for understanding the inception and development of wetlands and saline playa lakes under subtropical arid conditions.

Data availability. All the raw data can be provided by the corresponding authors upon request.

Author contributions. AJB, LM, MRR, FG and SM planned the campaign. SM, MRR, AJB and LM performed the measurements. AJB, MRR, LM, FG, IER, MD and KR analysed the data. AJB, FG, LM and MRR wrote the manuscript draft. IER, MDA and KR reviewed and edited the manuscript.

Competing interests. The contact author has declared that none of the authors has any competing interests.

Disclaimer. Publisher's note: Copernicus Publications remains neutral with regard to jurisdictional claims made in the text, published maps, institutional affiliations, or any other geographical representation in this paper. While Copernicus Publications makes every effort to include appropriate place names, the final responsibility lies with the authors.

Acknowledgements. We thank África Lupión (director of the Patronage of the Natural Reserve of Fuente de Piedra playa lake) for support during the field surveys and for providing historical monitoring data of the lake.

Financial support. This study was supported by the (1) tectonic conditioning and climate change effects on the hydrogeological evolution of wetlands and playa lakes in southern Spain research project (Pablo de Olavide University); (2) GYPCLIMATE research project (PID2021-123980OA-I00) of the Spanish Ministry of Economy and Competitiveness – Regional Development European Fund (FEDER); (3) PGC2018-100914-B-I00 project funded by the Ministerio de Ciencia e Innovacíon (Spanish government/AEI/10.13039/501100011033/ERDF); (4) UPO-1259543 project funded by the Consejería de Economía, Conocimiento, Compañías y Universidad (Andalusian government/ERDF) and (5) "Monitorizacion hidrológica y modelización de la relación laguna-acuífero en los mantos eólicos de Doñana. Seguimiento y ampliación del inventario" (agreement between the Guadalquivir River Basin Authority and Pablo de Olavide University). Fernando Gázquez acknowledges the Ramón y Cajal Scholarship (RYC2020-029811-I) and grant PPIT-UAL from the Junta de Andalucía-FEDER 2022–2026 (RyC-PPI2021-01). Lucía Martegani was funded by the

FPU21/06924 grant of the Ministerio de Educación y Formación Profesional of Spain.

Review statement. This paper was edited by Daniel Viviroli and reviewed by Martin Reiser and Blas Valero Garcés.

References

Allen, D. E., Singh, B. P., and Dalal, R. C.: Soil health indicators under climate change: a review of current knowledge, Soil Health Clim. Change, 29, 25–45, 2011.

Alonso-Zarza, A. M. and Wright, V. P.: Calcretes, Dev. Sedimentol., 61, 225–267, 2010.

Atalai, I.: Paleoenvironmental conditions of the Late Pleistocene and early Holocene in Anatolia, Turkey, in: Quaternary deserts and climate change, CRC Press, 227–237, eBook ISBN 9781003077862, 2020.

Balanya, J. C., Crespo-Blanc, A., Díaz-Azpiroz, M., Expósito, I., Torcal, F., Pérez-Peña, V., and Booth-Rea, G.: Arc-parallel vs back-arc extension in the Western Gibraltar arc: Is the Gibraltar forearc still active?, Geolog. Acta, 10, 249–263, 2012.

Barcos, L., Balanyá, J. C., Díaz-Azpiroz, M., Expósito, I., and Jiménez-Bonilla, A.: Kinematics of the Torcal Shear Zone: Transpressional tectonics in a salient-recess transition at the northern Gibraltar Arc, Tectonophysics, 663, 62–77, 2015.

Benavente, J., Carrasco, F., Almécija, C., Rodríguez-Jiménez, P., and Cruz Sanjulián, J.: La zona de transición agua dulce-salmuera bajo el borde norte de la laguna salada de Fuente de Piedra (Málaga), Geogaceta, 14, 6–8, 1993.

Berry, M., Van Wijk, J., Cadol, D., Emry, E., and Garcia-Castellanos, D.: Endorheic-exorheic transitions of the Rio Grande and East African rifts, Geochem. Geophy. Geosy., 20, 3705–3729, 2019.

Blaauw, M. and Christen, J. A.: Flexible paleoclimate age-depth models using an autoregressive gamma process, Bayesian Anal., 6, 457–474, https://doi.org/10.1214/11-BA618, 2011.

Camuera, J., Ramos-Román, M. J., Jiménez-Moreno, G., García-Alix, A., Ilvonen, L., Ruha, L., and Seppä, H.: Past 200 kyr hydroclimate variability in the western Mediterranean and its connection to the African Humid Periods, Sci. Rep., 12, 9050, https://doi.org/10.1038/s41598-022-12047-1, 2022.

Català, A., Cacho, I., Frigola, J., Pena, L. D., and Lirer, F.: Holocene hydrography evolution in the Alboran Sea: a multi-record and multi-proxy comparison, Clim. Past, 15, 927–942, https://doi.org/10.5194/cp-15-927-2019, 2019.

Cody, R. D. and Cody, A. M.: Gypsum nucleation and crystal morphology in analog saline terrestrial environments, J. Sediment. Res., 58, 247–255, 1988.

Cohen, T. J., Arnold, L. J., Gázquez, F., May, J. H., Marx, S. K., Jankowski, N. R., and Gadd, P.: Late quaternary climate change in Australia's arid interior: Evidence from Kati Thanda–Lake Eyre, Quaternary Sci. Rev., 292, 107635, https://doi.org/10.1016/j.quascirev.2022.107635, 2022.

Cruz-Sanjulián, J.: Mapa Geológico de Teba, 1 : 50.000, hoja no. 1.037, Instituto Tecnológico Geominero de España, Madrid, https://hdl.handle.net/20.500.14352/62998 (last access: 10 December 2024), 1991.

Díaz-Azpiroz, M., Barcos, L., Balanyá, J. C., Fernández, C., Expósito, I., and Czeck, D. M.: Applying a general triclinic transpression model to highly partitioned brittle-ductile shear zones: A case study from the Torcal de Antequera massif, external Betics, southern Spain, J. Struct. Geol., 68, 316–336, 2014.

Díaz Azpiroz, M., Asencio Almansa, R., Senín Andrades, J. R., and Jiménez Bonilla, A.: Shape preferred orientation of dolostone bodies of a Triassic broken formation at the western External Betics, Geogaceta, 67, 11–14, 2020.

Elez, J., Silva, P. G., Huerta, P., and Martínez-Graña, A.: Isostatic compensation in the Western-Central Betic Cordillera (South Spain) caused by erosional unloading from the Messinian to the present: the emergence of an orogen, Geogaceta, 64, 103–106, 2018.

Elez, J., Silva, P. G., and Martínez-Graña, A. M.: Quantification of Erosion and Uplift in a Rising Orogen – A Large-Scale Perspective (Late Tortonian to Present): The Case of the Gibraltar Arc, Betic Cordillera, Southern Spain, Remote Sens., 12, 3492, https://doi.org/10.3390/rs12213492, 2020.

Flinch, J. F. and Soto, J. I.: Allochthonous Triassic and salt tectonic processes in the Betic-Rif orogenic arc, in: Permo-Triassic salt provinces of Europe, North Africa and the Atlantic margins, Elsevier, 417–446, https://doi.org/10.1016/B978-0-12-809417-4.00020-3, 2017.

Flinch, J. F. and Soto, J. I.: Structure and Alpine tectonic evolution of a salt canopy in the western Betic Cordillera (Spain), Mar. Petrol. Geol., 143, 105782, https://doi.org/10.1016/j.marpetgeo.2022.105782, 2022.

García-Alix, A., Jiménez-Moreno, G., Gázquez, F., Monedero-Contreras, R., López-Avilés, A., Jiménez-Espejo, F. J., and Anderson, R. S.: Climatic control on the Holocene hydrology of a playa-lake system in the western Mediterranean, Catena, 214, 106292, https://doi.org/10.1016/j.catena.2022.106292, 2022.

Höbig, N., Mediavilla, R., Gibert, L., Santisteban, J. I., Cendón, D. I., Ibáñez, J., and Reicherter, K.: Palaeohydrological evolution and implications for palaeoclimate since the Late Glacial at Laguna de Fuente de Piedra, southern Spain, Quatern. Int., 407, 29–46, 2016.

Hughes, C. E. and Crawford, J.: Spatial and temporal variation in precipitation isotopes in the Sydney Basin, Australia, J. Hydrol., 489, 42–55, 2013.

Jiménez-Bonilla, A., Expósito, I., Balanyá, J. C., Díaz-Azpiroz, M., and Barcos, L.: The role of strain partitioning on intermontane basin inception and isolation, External Western Gibraltar Arc, J. Geodynam., 92, 1–17, 2015.

Jimenez-Bonilla, A., Torvela, T., Balanyá, J. C., Expósito, I., and Díaz-Azpiroz, M.: Changes in dip and frictional properties of the basal detachment controlling orogenic wedge propagation and frontal collapse: The external central Betics case, Tectonics, 35, 3028–3049, 2016.

Jiménez-Bonilla, A., Díaz-Azpiroz, M., and Rodríguez, M. R.: Tectonics may affect closed watersheds used to monitor climate change and human activity effects, Terra Nova, 35, 58–65, 2023a.

Jiménez-Bonilla, A., Rodríguez-Rodríguez, M., Yanes, J. L., and Gázquez, F.: Hydrological modelling and evolution of lakes and playa-lakes in southern Spain constrained by geology, human management and climate change, Sci. Total Environ., 905, 167183, https://doi.org/10.1016/j.scitotenv.2023.167183, 2023b.

Jiménez-Bonilla, A., Díaz-Azpiroz, M., Rodríguez-Rodríguez, M., Balanyá, J. C., and Expósito, I.: Tectonic Controls on Drainage Network, Topographic Barriers Building and the Development of Endorheic Areas in the Western Betics (S Spain), Implications on the Evolution of the Atlantic-Mediterranean Water Divide, in preparation, 2024.

Kohfahl, C., Sprenger, C., Herrera, J. B., Meyer, H., Chacón, F. F., and Pekdeger, A.: Recharge sources and hydrogeochemical evolution of groundwater in semiarid and karstic environments: A field study in the Granada Basin (Southern Spain), Appl. Geochem., 23, 846–862, 2008.

Linares, L.: Hydrogeology of Fuente de Piedra lake (Málaga), PhD Thesis Dissertation, University of Granada, 343 pp., 1990.

Macumber, P. G.: Hydrological processes in the Tyrrell Basin, southeastern Australia, Chem. Geol., 96, 1–18, 1992.

Mann, M., Amman, C., Bradley, R., Briffa, K., Jones, P., Osborn, T., and Wigley, T.: On past temperatures and anomalous late-20th-century warmth, Eos Trans. Am. Geophys. Union, 84, 256–256, 2003.

Martos-Rosillo, S., González-Ramón, A., Jiménez-Gavilán, P., Andreo, B., Durán, J. J., and Mancera, E.: Review on groundwater recharge in carbonate aquifers from SW Mediterranean (Betic Cordillera, S Spain), Environ. Earth Sci., 74, 7571–7581, 2015.

Matthews, J., Anderson, S., Geoghegan, T., Ayers, J., Warner, K., Fieldman, G., and Falloon, P.: Evapotranspiration in a warming climate: Model uncertainty and role for climate adaptation, IOP Conf. Ser.: Earth Environ. Sci., 6, 052014, https://doi.org/10.1088/1755-1307/6/5/052014, 2008.

Moral, F., Rodriguez-Rodriguez, M., Beltrán, M., Benavente, J., and Cifuentes, V. J.: Water regime of Playa Lakes from southern Spain: conditioning factors and hydrological modeling, Water Environ. Res., 85, 632–642, 2013.

Moral Martos, F.: Caracterización y origen de las lunetas asociadas a las lagunas de La Lantejuela (Sevilla, España), Geogaceta, 59, 3–6, 2016.

Morcillo-Montalbá, L., Rodrigo-Gámiz, M., Martínez-Ruiz, F., Ortega-Huertas, M., Schouten, S., and Sinninghe Damsté, J. S.: Rapid Climate Changes in the Westernmost Mediterranean (Alboran Sea) Over the Last 35 kyr: New Insights From Four Lipid Paleothermometers (UK'37, TEXH86, RI-OH', and LDI), Paleoceanogr. Paleoclimatol., 36, e2020PA004171, https://doi.org/10.1029/2020PA004171, 2021.

Obert, J. C., Muenker, C. Staubwasser, M., Herwartz, D., Reicherter, K., and Chong, G.: ^{230}Th dating of gypsum from lacustrine, brackish-marine and terrestrial environments, Chemical Geol., 607, 121019, https://doi.org/10.1016/j.chemgeo.2022.121019, 2022.

Reimer, P. J., Austin, W. E. N., Bard, E., Bayliss, A., Blackwell, P. G., Bronk Ramsey, C., Butzin, M., Cheng, H., Edwards, R. L., Friedrich, M., Grootes, P. M., Guilderson, T. P., Hajdas, I., Heaton, T. J., Hogg, A. G., Hughen, K. A., Kromer, B., Manning, S. W., Muscheler, R., Palmer, J. G., Pearson, C., van der Plicht, J., Reimer, R. W., Richards, D. A., Scott, E. M., Southon, J. R., Turney, C. S. M., Wacker, L., Adolphi, F., Büntgen, U., Capano, M., Fahrni, S. M., Fogtmann-Schulz, A., Friedrich, R., Köhler, P., Kudsk, S., Miyake, F., Olsen, J., Reinig, F., Sakamoto, M., Sookdeo, A. and Talamo, S.: The IntCal20 Northern Hemisphere Radiocarbon Age Calibration Curve (0–55 cal kBP), Radiocarbon, 62, 725–757, 2020.

Roberts, N., Reed, J. M., Leng, M. J., Kuzucuoğlu, C., Fontugne, M., Bertaux, J., and Karabiyikoğlu, M.: The tempo of Holocene climatic change in the eastern Mediterranean region: new high-resolution crater-lake sediment data from central Turkey, Holocene, 11, 721–736, 2001.

Rodríguez-Hernández, L., Hernández-Bravo, J. C., and Fernández-Mejuto, M.: Processing and management of hidrologic time series: user manual: application, TRASERO, Diputación de Alicante, Ciclo Hídrico, https://ciclohidrico.com/download/tratamiento-y-gestion-de-series-temporales-hidrologicas/trasero/ (last access: 10 December 2024), 2007.

Rodríguez-Rodríguez, M., Moral, F., Benavente, J., and Beltrán, M.: Developing hydrological indices in semi-arid playa-lakes by analyzing their main morphometric, climatic and hydrochemical characteristics, J. Arid Environ., 74, 1478–1486, 2010.

Rodríguez-Rodríguez, M., Green, A. J., López, R., and Martos-Rosillo, S.: Changes in water level, land use, and hydrological budget in a semi-permanent playa lake, Southwest Spain, Environ. Monit. Assess., 184, 797–810, 2012.

Rodríguez-Rodríguez, M., Martos-Rosillo, S., Pedrera, A., and Benavente-Herrera, J.: Ratosa playa lake in southern Spain. Karst pan or compound sink?, Environ. Monit. Assess., 187, 1–15, 2015.

Rodríguez-Rodríguez, M., Martos-Rosillo, S., and Pedrera, A.: Hydrogeological behaviour of the Fuente-de-Piedra playa lake and tectonic origin of its basin (Malaga, southern Spain), J. Hydrol., 543, 462–476, 2016.

Sánchez-Moral, S., Ordóñez, S., Benavente, D., and del Cura, M. G.: The water balance equations in saline playa lakes: comparison between experimental and recent data from Quero Playa Lake (central Spain), Sediment. Geol., 148, 221–234, 2002.

Sandler, A., Meunier, A., and Velde, B.: Mineralogical and chemical variability of mountain red/brown Mediterranean soils, Geoderma, 239, 156–167, 2015.

Schröder, T., van't Hoff, J., López-Sáez, J. A., Viehberg, F., Melles, M., and Reicherter, K.: Holocene climatic and environmental evolution on the southwestern Iberian Peninsula: a high-resolution multi-proxy study from Lake Medina (Cádiz, SW Spain), Quaternary Sci. Rev., 198, 208–225, 2018.

Schröder, T., López-Sáez, J. A., van't Hoff, J., and Reicherter, K.: Unravelling the Holocene environmental history of southwestern Iberia through a palynological study of Lake Medina sediments, Holocene, 30, 13–22, 2020.

Vera, J. A. (Ed.): Geología de españa, IGME – Instituto Geológico y Minero de España, ISBN 84-7840-546-1, 2004.